Highly-efficient cryogenic Yb:YLF regenerative amplifier with 250 W average power

UMIT DEMIRBAS,[1,4,*] MARTIN KELLERT,[1] JELTO THESINGA,[1] YI HUA,[1] SIMON REUTER,[1] MIKHAIL PERGAMENT[1] AND FRANZ X. KÄRTNER[1,2,3]

[1]Center for Free-Electron Laser Science, Deutsches Elektronen-Synchrotron DESY, Notkestraße 85, 22607 Hamburg, Germany
[2]Physics Department, University of Hamburg, Luruper Chaussee 149, 22761 Hamburg, Germany
[3]The Hamburg Centre for Ultrafast Imaging, Luruper Chaussee 149, 22761 Hamburg, Germany
[4]Laser Technology Laboratory, Department of Electrical and Electronics Engineering, Antalya Bilim University, 07190 Dosemealti, Antalya, Turkey
*uemit.demirbas@cfel.de

Received XX Month XXXX; revised XX Month, XXXX; accepted XX Month XXXX; posted XX Month XXXX (Doc. ID XXXXX); published XX Month XXXX

We report an efficient diode-pumped high-power cryogenic regenerative amplifier operating at 1019 nm employing the c-axis of Yb:YLF. Compared to the usually selected 1017 nm transition of a-axis, the c-axis 1019 nm line has 3-fold higher emission cross section and still possess a full-width-half-maximum (FWHM) of 6.5 nm at 125 K. The chirped-pulse amplifier system is seeded by a fiber front-end with an energy of 30 nJ and stretched pulsewidth of 2 ns. In regenerative amplification studies, using the advantage of higher gain in the c-axis, we have achieved record average powers up to 370 W, with an extraction efficiency of 78% at 50 kHz repetition rate. The output pulses were centered around 1019.15 nm with a FWHM bandwidth of 1.25 nm, which supports sub-1.5 ps pulse durations. The output beam maintained a TEM_{00} beam profile at output power levels below 250 W with an M^2 below 1.2. Above this power level the thermally induced lensing in Yb:YLF created a multimode output beam. The thermal lens was rather dynamic and deteriorated the system stability above 250 W average power level.

http://dx.doi.org/10.1364/OL.99.099999

Continuous-wave (cw) lasing of Yb:YLF was first reported in 2001, where a simple 400 mW diode-pumped system produced 50 mW of output power in the 1025-1050 nm range [1]. Benefits of cryogenic cooling were already discussed in this initial work [1], and lasing at cryogenic temperatures was shown only a year later [2]. Over the past 20 years, output power of cryogenic ($Yb:LiYF_4$) laser systems evolved from 100 mW to 500 W level [2–7]. Interestingly, as it is underlined by Kawanaka et al. in their pioneering work [1], the Yb:YLF gain media possess broad emission bands even at cryogenic temperatures [8–10]. Especially, the a-axis of Yb:YLF, which has a transition centered around 1016-1017 nm with a FWHM of 11 nm at 125 K (typical operation temperature of Yb:YLF amplifiers under thermal load [11]), could ideally support generation and amplification of sub-250-fs pulses [3]. Because of its broad emission profile, almost all cryogenic amplification studies with Yb:YLF so far had employed the a-axis, and amplification of sub-ps pulses with energies up to 300 mJ, and average powers up to 100 W was already demonstrated [12–16].

However, the c-axis of Yb:YLF has stronger but narrower transitions [8–10]. Specifically, the peak at 995.2 nm has very high gain (small-signal single-pass gain above 50) [8], but it has a rather narrow width of only 0.5-0.75 nm at 78 K, which extends to around 2 nm at 125 K. In a recent study, Manni et al. demonstrated first cryogenic amplification using this line, where 1 μs long 60 nJ pulses at 995 nm were amplified to 1 mJ level (repetition rate: 40 kHz, average power: 40 W) [17]. The c-axis of Yb:YLF has another strong line centered around 1019 nm, which to our knowledge, was not explored in any cryogenic amplification study yet. The 1019 nm line of Yb:YLF has a FWHM of 3.7 nm at 78 K, which extends to a FWHM of 6.5 nm at 125 K [8]. This line is not as broad as the 1017 nm transition of E//a axis, but it has around 3 times higher emission cross section [8]. In this Letter, to the best of our knowledge, we report first amplification results with the 1019 nm transition of E//c axis in Yb:YLF. With the advantage of higher gain, we have demonstrated an extraction efficiency of 78% and an average power of 370 W from the amplifier, which are to our knowledge, record results for a cryogenic Yb:YLF system.

Figure 1 (a) shows a simplified schematic for the Yb:YLF regenerative amplifier. A 2-kW, 960 nm diode module was used as the pump source. Imaging lenses (f1-f3) were employed to achieve a 2.1 mm diameter pump spot at the center of the Yb:YLF crystal. A 2 cm long 1% Yb-doped YLF crystal with 3-mm long undoped endcaps diffusion-bonded on both ends was used as the gain medium. The crystal was indium bonded from the top side to a cold

head, which was cooled to cryogenic temperatures by liquid nitrogen. The c-axis of the crystal was positioned vertically to benefit from its higher thermal conductivity [18]. The crystal absorbed around 85 % of the incident pump light at 960 nm. The bow-tie type regenerative ring cavity had a total length of 3 m, and consisted of two dichroic mirrors (DM) with a radius of curvature of 20 m and two flat high reflectors. The reflectivity of the cavity mirrors covered the 990-1230 nm spectral range. Two thin-film polarizer's (TFPs), a half-wave plate (HWP) and a water-cooled 8-mm aperture BBO Pockell cell (PC) with a rise (fall) time of 8 ns (3.5 ns) were used for seeding of the amplifier. Two additional HWPs were implemented to employ the E//c axis for amplification. The cold cavity had a calculated beam diameter of around 2.2 mm and 2.15 mm at the center of the Yb:YLF crystal and PC, respectively. The system is seeded by stretched (2 ns) pulses with 30 nJ energy from a fiber front-end [19]. The total passive loss of the cold cavity is measured to be around 5%: 2.5% from the Yb:YLF dewar (crystal and dewar windows), 1% depolarization loss and the rest from all the remaining elements. A simpler standing-wave cavity, as shown in Fig. 1 (b), was also used to benchmark the cw laser performance of the system. The beam parameters of the standing-wave cw cavity was almost identical to the regenerative amplifier.

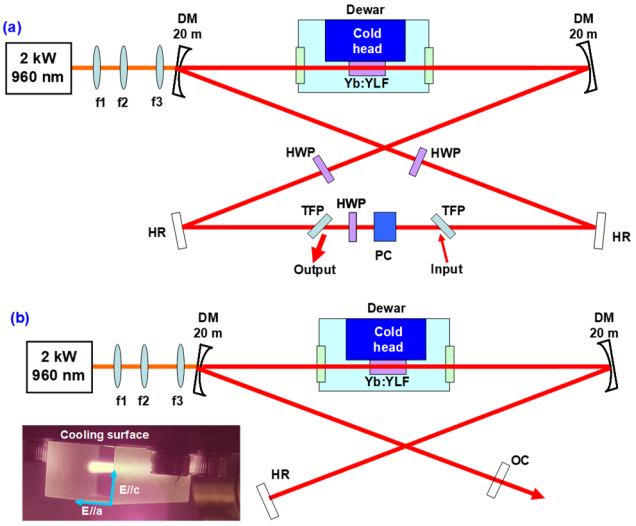

Fig. 1. (a) Experimental setup of the diode-pumped cryogenic Yb:YLF regenerative amplifier. (b) Setup for a simple standing-wave Yb:YLF laser with identical cavity beam parameters. Inset picture shows the Yb:YLF crystals orientation.

We present the cw lasing results first, since the limitations observed for the simpler cw cavity are quite informative in understanding the limitations observed in the regenerative amplifier performance. For that purpose, Fig. 2 (a) shows the cw laser efficiency data taken using a 40% transmitting output coupler. The laser had a cw lasing threshold of 45 W, a slope efficiency of 76%, and generated an output power of 506 W at an absorbed pump power of 780 W (850 W incident). The estimated temperature of the Yb:YLF crystal (±10 K) is also shown in Fig. 2 (a) [20]. The free running cw laser wavelength was 995 nm for an absorbed pump just below 300 W. Then the wavelength switched to the 1019 nm line for pump powers above 300 W [6]. The change in lasing wavelength with absorbed power is due to the induced variation in crystal temperature: at higher temperatures due to Boltzmann redistribution of level populations, the gain cross section at 1019 nm line becomes larger than that of 995 nm transition (see Figs. 2 and 5 in [8]).

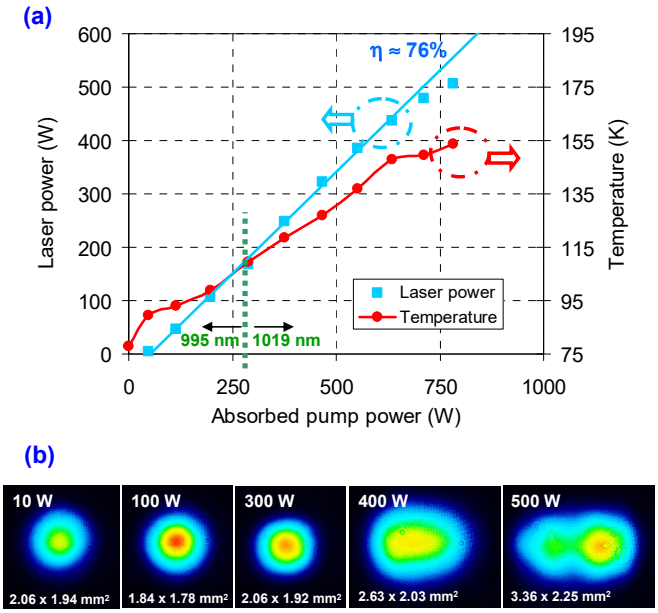

Fig. 2. (a) Measured cw laser performance of the cryogenic Yb:YLF laser using a 40% transmitting output coupler. Measured average temperature of the crystal is also shown. The free running laser wavelength switched from 995 nm to 1019 nm at an absorbed pump power of around 300 W. (b) Near-field beam profiles of the cw Yb:YLF cryogenic laser at different output power levels.

The achievable cw laser power was limited by thermal lensing effects as is also visible from the bending of the cw efficiency curve. For absorbed pump power levels above 500 W, the thermally induced lensing in the crystal gradually deteriorated the output beam profile as shown in Fig. 2 (b) [6]. Once the absorbed pump reached 750 W level, the thermal lens become rather dynamic and it was not possible to optimize the laser with further re-alignment (a reduction in output power is also observed). As can be seen from the behavior of laser output near-field for different output power levels, the output beam elongates along the horizontal direction, the a-axis (beam size increases from around 2.1 mm to 3.4 mm). On the other hand, the beam shape did not change significantly in the vertical direction (stayed around ~2 mm), the c-axis. The thermal coefficient of refractive index (dn/dT) is negative for both axis of Yb:YLF [18], which provides a significant advantage to YLF as a laser host for power-scaling compared to other well-known host materials like YAG [21]. Basically, the negative contribution of dn/dT is cancelled by other contributions to thermal lensing such as surface bulging and one ends up with a small overall thermal lens. For the c-axis, the dn/dT parameter of YLF has a larger value (-2.5 ppm/K in c-axis versus -1 ppm/K in a-axis, for a temperature of 150 K: Fig. 23 in [18]). We believe that, the larger negative value of dn/dT of the c-axis is the main reason for the better thermal lensing performance observed in the vertical axis (c-axis) in our study. As a side note, with Yb:YAG, due to its positive dn/dT parameter, a much stronger thermal lens exists at similar absorbed pump power levels.

As a result, we could only achieve a cw power of 100 W from an identical laser cavity with Yb:YAG (using a 25 mm long 1% Yb-doped YAG sample, pumped with a similar diode module at 940 nm). A short cavity with better immunity to thermal lensing was required to achieve higher powers from Yb:YAG rod (365 W cw power at 480 W of absorbed power). Hence, the cw output power obtainable with cryogenic Yb:YLF from a single rod [6], is already significantly higher than what can be achieved with cryogenic Yb:YAG systems under similar conditions.

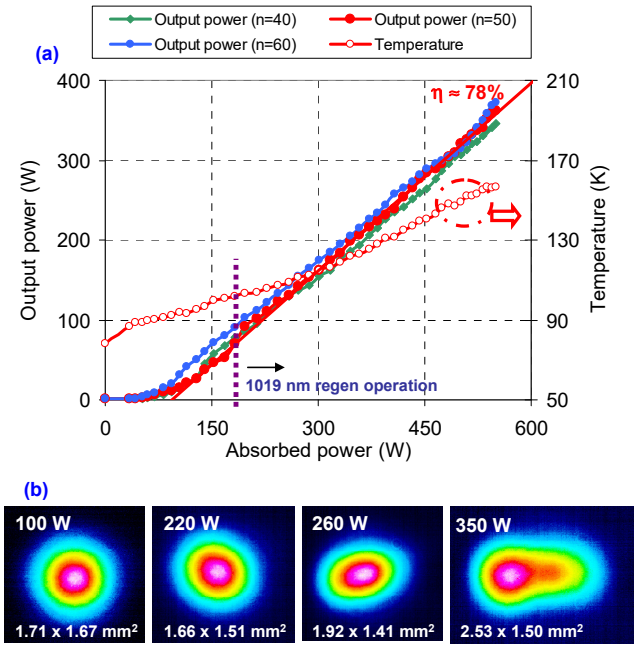

Fig. 3. (a) Measured output power of the Yb:YLF regenerative amplifier as a function of absorbed pump power at 50 kHz repetition rate. The data is taken for different cavity round-trips (n) of 40, 50 and 60, using a seed energy of 30 nJ. The measured average temperature of the crystal is also shown. (b) Sample near-field beam profiles of the Yb:YLF regenerative amplifier at different output power levels showing the increased role of thermal lensing on beam profile.

Figure 3 (a) shows the measured performance of the Yb:YLF regenerative amplifier for cavity round-trips (n) of 40, 50 and 60, at a repetition rate of 50 kHz. First of all, as we also observed in cw laser experiments, for low absorbed pump power and hence low crystal temperatures, the gain at 995 nm is very strong [8], and the system started parasitic cavity-dumped lasing at 995 nm with sub-10-ns pulse width even when seeded with 30 nJ pulses at 1019 nm. With the heating of the crystal, the parasitic 995 nm lasing was fully suppressed for absorbed pump power levels above 170 W (for larger n the suppression starts earlier). The regenerative amplifier produced up to 373 W of average power at an absorbed pump power of 550 W (incident power 708 W) for the case with 60 round trips. A linear fit to the data shows that the efficiency of the amplifier is as high as 78%, which is rather close to the quantum defect limited operation (94%: 960 nm /1019 nm). Note that, at this repetition rate, the system operates in saturated mode, as there is only a minor difference in amplifier performance for cavity round trips of n=40, 50 and 60. We have also tested the variation of output power with seed energy, and saw a decrease of only 15% in output power when the seed energy was lowered from 40 nJ to 0.2 nJ at a fixed round-trip number of 50. With an even stronger seed, the parasitic lasing at 995 nm is suppressed earlier, and the number of round trips of the regenerative amplifier could be reduced to around 20 to increase system stability. Similar to the cw case, the regenerative amplifier performance was limited due to the thermal lensing effect. Fig. 3 (b) shows the output beam profile of the amplifier at different average output power levels. The output beam had a rather symmetric TEM_{00} beam profile for power levels below 250 W. At these power levels, the beam quality (M^2) of the output was measured to be below 1.2 for both axes [6,16] . For output power levels above 300 W, the thermally induced lensing in Yb:YLF created a multimode output beam. Also, the thermal lens was rather dynamic and created system stability issues at these power levels (250-350 W). Interestingly, the thermal lensing limited the output power earlier in the regenerative amplifier compared to the cw cavity. We believe this is related to the larger number of round-trips required for the regenerative amplifier (in the cw laser with 40% OC, the photon on average has 4 passes through the crystal). Despite that, in its current form, safe long-term operation of the system was feasible for an output power up to 250 W, and higher power might be sustainable via active intracavity beam pointing control.

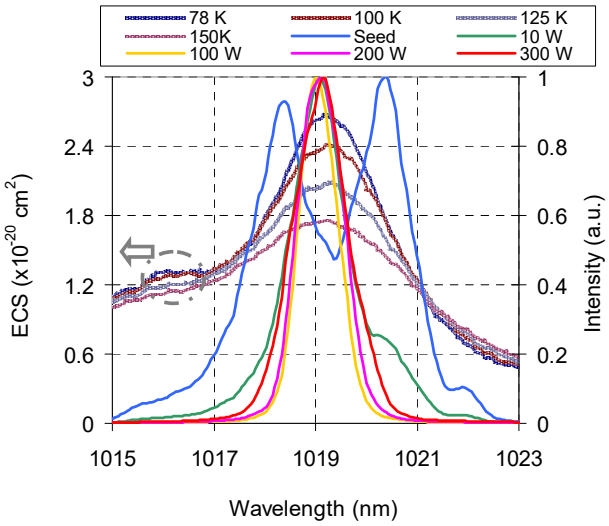

Fig. 4. Optical spectrum of seed pulse and regenerative amplifier output pulse at average output power levels of 10 W, 100 W, 200 W and 300 W. The data is taken at a pulse repetition rate of 50 kHz, using 30 nJ seed energy and with 50 round trips (n=50). The measured emission cross section (ECS) for the E//c axis of Yb:YLF is also shown for crystal temperatures of 78 K, 100 K, 125 K and 150K.

Figure 4 shows the measured optical spectrum of the seeder as well as the amplifier output at different average power levels. The seeder was centered around 1019.5 nm and had HWHM of 3.3 nm. With amplification, the spectrum first narrowed down to a width of 0.9 nm at 100 W power level, but then started to broaden again due to increased crystal temperature and smoother gain profile. Fig. 4 also contains the measured emission cross section of the c-axis of Yb:YLF at selected temperatures, where we can easily observe the effect of temperature in smoothing out the gain profile [8]. At an output power level of 300 W, the spectra were centered around 1019.15 nm with a FWHM bandwidth of 1.25 nm, which could support sub-

1.5 ps pulse duration. It is clear that, via usage of intracavity filters, sub-1-ps pulse durations might be achievable from the 1019 nm line of E//c axis of Yb:YLF in future studies.

In Figure 5, we show the measured amplifier performance at 25, 50 and 100 kHz repetition rate for a fixed cavity round trip number of 50. As expected, we could achieve similar amplification performance for each repetition rate (similar average powers, reduced pulse energy at higher repetition rates) [22]. For the 25 kHz repetition rate, we stopped at 250 W (10 mJ energy) on purpose to stay away from laser induced damage to the cavity optics in this first trial as replacement elements were not available on site. For the ~1.6 mm beam, the 10 mJ energy corresponds to a peak fluence of 1 J/cm^2. Due to gain narrowing, the pulsewidth of the output pulses was reduced from around 2 ns to 1.25-1.5 ns, and we know from earlier experience that, the fluence values could be safely scaled up to 2 J/ cm^2 for such pulses: hence ideally pulse energies of 20 mJ are safely achievable from this system.

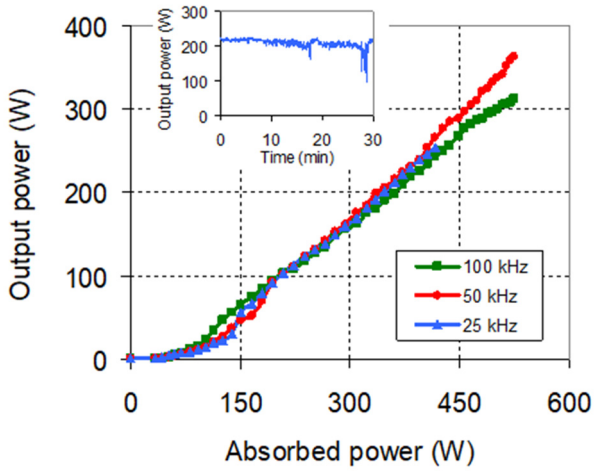

Fig. 5. Measured output power performance of the Yb:YLF regenerative amplifier at 25 kHz, 50 kHz and 100 kHz repetition rate. The data is taken at 50 cavity round-trips, using 30 nJ seed energy. The inset shows the variation of measured average output power of the regen at 220 W for 30 minutes (50 kHz case).

To finalize, the inset graph in Fig. 5 shows the measured average output power of the amplifier for a 30 minute interval at an average power level of around 220 W. The data is taken without enclosing the cavity. The power fluctuations were measured to be below 3% rms in the first 8 minutes. The changing level of liquid nitrogen in the Yb:YLF dewar created the fluctuations over longer time scales, which can be resolved by installing a liquid nitrogen auto-refill system or a closed-cycle cooler (the small dip in the curve is a realignment effort).

In summary, we have presented, to the best of our knowledge, the first Yb:YLF amplifier employing the 1019 nm transition of the c-axis. The higher gain compared to the a-axis enabled a system with record average power and extraction efficiency. The thermally induced lensing in Yb:YLF is shown to be the main limitation for further power scaling. As the estimated B-integral of the system is still low (below 0.5), in future studies, usage of longer Yb:YLF crystals with lower doping (0-5-0.75% Yb-doped 3-4 cm long) could reduce the thermal lensing issue induced in this work. Further average power scaling might be feasible via usage of periodic resonators with multiple gain elements [22,23] or via usage of zig-zag slab or thin disk geometries.

Funding. Seventh Framework Programme (FP7) FP7/2007- 2013 European Research Council (ERC) Synergy Grant (609920).

Acknowledgment. The authors acknowledge support from previous group members L. E. Zapata, K. Zapata for establishing the indium-bonding technology for YLF at CFEL-DESY.

Disclosures. The authors declare no conflicts of interest.

References

1. J. Kawanaka, H. Nishioka, N. Inoue, and K. Ueda, Appl. Opt. **40**, 3542 (2001).
2. J. Kawanaka, K. Yamakawa, H. Nishioka, and K. Ueda, Opt. Express **10**, 455 (2002).
3. J. Kawanaka, S. Tokita, H. Nishioka, M. Fujita, K. Yamakawa, K. Ueda, and Y. Izawa, Laser Phys. **15**, 1306 (2005).
4. L. E. Zapata, D. J. Ripin, and T. Y. Fan, Opt. Lett. **35**, 1854 (2010).
5. N. Ter-Gabrielan, V. Fromzel, T. Sanamyan, and M. Dubinskii, Opt. Mater. Express **7**, 2396 (2017).
6. M. Kellert, U. Demirbas, J. Thesinga, S. Reuter, M. Pergament, and F. X. Kärtner, Opt. Express **29**, 11674 (2021).
7. U. Demirbas, H. Cankaya, J. Thesinga, F. X. Kärtner, and M. Pergament, Opt. Express **27**, (2019).
8. U. Demirbas, J. Thesinga, M. Kellert, F. X. Kärtner, and M. Pergament, Opt. Mater. Express **11**, (2021).
9. S. Püschel, S. Kalusniak, C. Kränkel, and H. Tanaka, Opt. Express **29**, 11106 (2021).
10. J. Korner, M. Kruger, J. Reiter, A. Munzer, J. Hein, and M. C. Kaluza, Opt. Mater. Express **10**, 2425 (2020).
11. U. Demirbas, M. Kellert, J. Thesinga, Y. Hua, S. Reuter, F. X. Kärtner, and M. Pergament, Appl. Phys. B **127**, 46 (2021).
12. D. Rand, D. Miller, D. J. Ripin, and T. Y. Fan, Opt. Mater. Express **1**, 434 (2011).
13. J. Kawanaka, K. Yamakawa, H. Nishioka, and K. Ueda, Opt. Lett. **28**, 2121 (2003).
14. D. E. Miller, L. E. Zapata, D. J. Ripin, and T. Y. Fan, Opt. Lett. **37**, 2700 (2012).
15. Y. Z. Liu, U. Demirbas, M. Kellert, J. Thesinga, H. Cankaya, Y. Hua, L. E. Zapata, M. Pergament, and F. X. Kartner, Osa Contin. **3**, 2722 (2020).
16. U. Demirbas, H. Cankaya, Y. Hua, J. Thesinga, M. Pergament, and F. X. Kärtner, Opt. Express **28**, (2020).
17. J. Manni, D. Harris, and T. Y. Fan, Opt. Commun. **417**, 54 (2018).
18. R. L. Aggarwal, D. J. Ripin, J. R. Ochoa, and T. Y. Fan, J. Appl. Phys. **98**, (2005).
19. Y. Hua, W. Liu, M. Hemmer, L. E. Zapata, G. J. Zhou, D. N. Schimpf, T. Eidam, J. Limpert, A. Tunnermann, F. X. Kartner, and G. Q. Chang, Opt. Lett. **43**, 1686 (2018).
20. U. Demirbas, J. Thesinga, M. Kellert, F. X. Kärtner, and M. Pergament, Opt. Mater. Express **10**, 3403 (2020).
21. D. J. Ripin, J. R. Ochoa, R. L. Aggarwal, and T. Y. Fan, Opt. Lett. **29**, 2154 (2004).
22. U. Demirbas, H. Cankaya, J. Thesinga, F. X. Kärtner, and M. Pergament, J. Opt. Soc. Am. B **37**, 1865 (2020).
23. J. M. Eggleston, IEEE J. Quantum Electron. **24**, 1821 (1988).